



**A NEW MEASUREMENT OF DIRECT CP VIOLATION IN THE
NEUTRAL KAON SYSTEM**

G.D. Barr, P. Buchholz, R. Carosi, D. Coward^{1,2}, D. Cundy, N. Doble, L. Gatignon,
V. Gibson³, P. Grafström, R. Hagelberg, J. van der Lans, H.N. Nelson⁴, H. Wahl
CERN, Geneva, Switzerland

K.J. Peach

Physics Department, University of Edinburgh, Edinburgh, UK

H. Blümer, R. Heinz, K. Kleinknecht, P. Mayer, B. Panzer⁵, B. Renk, H. Rohrer,
H.G. Sander, A. Wagner

Institut für Physik, Universität Mainz, Mainz, Germany⁶

E. Augé, D. Fournier, P. Heusse, L. Iconomidou-Fayard, I. Harrus, O. Perdereau,
A.C. Schaffer, L. Serin

*Laboratoire de l'Accélérateur Linéaire, IN2P3-CNRS, Université de Paris-Sud, Orsay,
France⁷*

L. Bertanza, A. Bigi, P. Calafiura⁸, M. Calvetti⁹, M.C. Carozza, R. Casali, C. Cerri,
R. Fantechi, I.G. Mannelli⁸, V.M. Marzulli⁸, A. Nappi¹⁰, G. Pierazzini
Dipartimento di Fisica e Sezione INFN di Pisa, Pisa, Italy

M. Holder, A. Kreutz, G. Quast¹¹, M. Rost, R. Werthenbach, G. Zech
Fachbereich Physik, Universität Siegen, Siegen, Germany¹²

Abstract

A new measurement of the ratio of the CP-violating amplitudes for $K_L \rightarrow 2\pi^0$ and $K_L \rightarrow \pi^+\pi^-$ is reported. The measured value for $R = |\eta_{00}/\eta_{+-}|^2$ is $0.9878 \pm 0.0026 \pm 0.0030$, where the first error is the statistical uncertainty and the second is the estimate of the systematic uncertainty. This gives a value for the parameter describing direct CP violation: $\text{Re } \epsilon'/\epsilon = (2.0 \pm 0.7) \times 10^{-3}$.

(Submitted to Physics Letters)

Introduction

The twenty-nine years since the experimental discovery of CP violation in the neutral kaon system have seen great progress in both the experimental techniques used to study this phenomenon and the theoretical interpretation of the measurements. Whilst there is general agreement [1] on the magnitude of CP violation in the kaon mass-matrix, recent precision measurements [2, 3] on the relative amounts of CP violation in the transition to the two possible 2π final states differ at the two standard deviation level. In the earlier result [2] from this Collaboration, evidence for direct CP violation was reported, $R = |\eta_{00}/\eta_{+-}|^2 = 0.980 \pm 0.004 \pm 0.005$, and $\text{Re } \epsilon'/\epsilon = (3.3 \pm 1.1) \times 10^{-3}$, whilst a more recent measurement [3], $\text{Re } \epsilon'/\epsilon = (0.74 \pm 0.59) \times 10^{-3}$, is consistent with no effect.

The result reported here is a new measurement of $\text{Re } \epsilon'/\epsilon$ using the same method as reference [2] with data taken in both 1988 and 1989. The data sample is about three times that of reference [2], of which two thirds was obtained in 1989. There have been significant improvements to the beam and the detector in order to understand the backgrounds better and to reduce the systematic uncertainties. In the following, the method, the beam, and the detector are described briefly, with emphasis on the differences from the previous measurement. Subsequently, the data selection and analysis are presented. A more detailed description of the beam and detector can be found in reference [4], and a full discussion of the present experimental results will be given in reference [5].

Overview of the method

Collinear neutral beams created by high-energy protons striking beryllium targets are alternately used to generate quite similar distributions of K_L and K_S two-pion decays over a 50 m fiducial region. Measurement of the decays is based on large-acceptance wire chambers and calorimeters, located about 120 m from the beginning of the fiducial region. The K_L energy spectrum peaks at 100 GeV and the decay vertex distribution is essentially flat ($\gamma c\tau_{K_L} \simeq 3$ km). The decay vertex distribution for K_S decays ($\gamma c\tau_{K_S} \simeq 5$ m) is made similar to that for the K_L decays by mounting the K_S target and collimator on a train which can be positioned at 41 stations, separated by 1.2 m, throughout the 50 m fiducial region. The K_S energy spectrum is naturally somewhat harder than the K_L spectrum because of K_S decays occurring before the collimator and the probability for K_L to decay in the fiducial region. This difference is partially compensated by the choice of a lower proton beam energy and larger production angle for the K_S beam. Figures 1a and 1b show the measured energy spectra and vertex distributions of the four decay modes.

¹⁾ On leave from SLAC, Stanford, CA 94309, USA

²⁾ Work supported in part by the US Department of Energy contract DE-AC03-76F00515

³⁾ Present address: University of Cambridge, Cambridge CB3 9EW, UK

⁴⁾ Present address: University of California at Santa Barbara, CA 93106, USA

⁵⁾ Present address: CERN, Geneva, Switzerland

⁶⁾ Funded by the German Federal Minister for Research and Technology (BMFT) under contract 054Mz18

⁷⁾ Funded by Institut National de Physique des Particules et de Physique Nucléaire (IN2P3), France

⁸⁾ Present address: Scuola Normale Superiore, Pisa, Italy

⁹⁾ Present address: Dipartimento di Fisica e Sezione INFN, Perugia, Italy

¹⁰⁾ Present address: Dipartimento di Scienze Fisiche, University of Cagliari, Cagliari, Italy

¹¹⁾ Present address: Institut für Experimentalphysik der Universität Hamburg, W-2000 Hamburg 52, Germany

¹²⁾ Funded by the German Federal Minister for Research and Technology (BMFT) under contract 054Si74

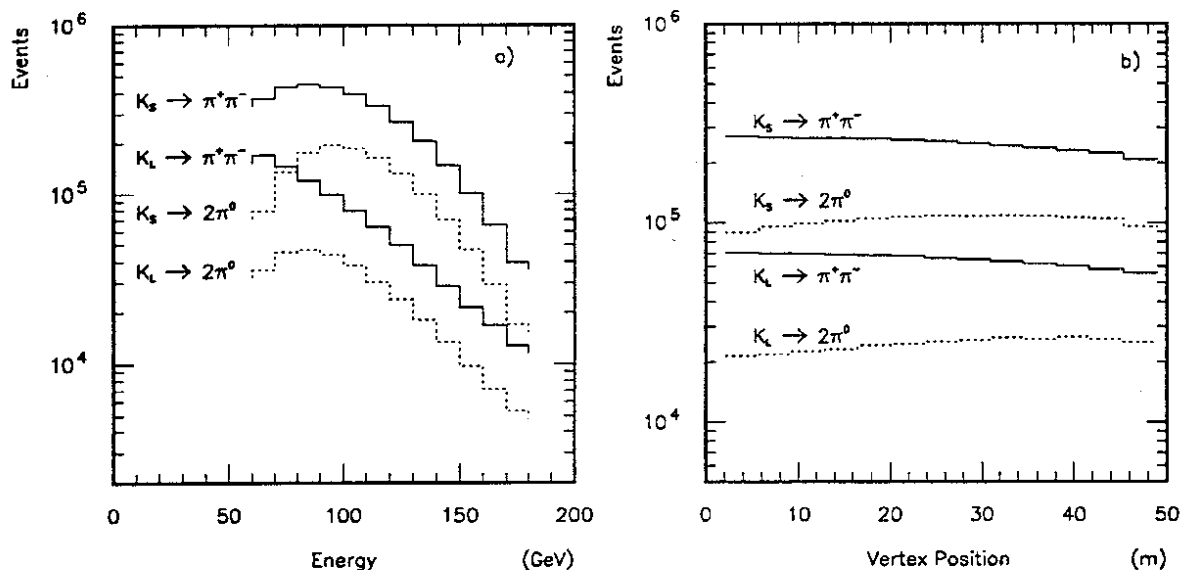


Figure 1: The energy spectra (a) and the vertex distributions (b) of the $\pi^+\pi^-$ and $\pi^0\pi^0$ decay modes in the K_S and K_L beams. Events in K_S have been weighted as a function of target position so that the K_S and K_L vertex distributions are nearly identical.

Events are collected concurrently in both the charged ($\pi^+\pi^-$) and neutral ($\pi^0\pi^0$) modes. In the K_L beam, the dominant three-body decays are reduced to a background subtraction at the per-cent level through particle identification and kinematic cuts; background in the K_S beam is less than 10^{-3} and is thus negligible. In order to extract $\text{Re } \epsilon'/\epsilon$, the double ratio R of CP-violating to CP-conserving 2π decay rates,

$$R \equiv \frac{\Gamma(K_L \rightarrow 2\pi^0) / \Gamma(K_L \rightarrow \pi^+\pi^-)}{\Gamma(K_S \rightarrow 2\pi^0) / \Gamma(K_S \rightarrow \pi^+\pi^-)} = 1 - 6 \text{Re } \epsilon'/\epsilon,$$

is formed in bins of energy and decay position to minimize the acceptance correction. There are small corrections to the double ratio of observed decays owing to the residual differences in acceptance, measurement resolution, trigger efficiency, and the efficiency of the K_S anti-counter used to define the beginning of the K_S fiducial region. A few per cent of events are lost in each beam because of unassociated additional activity in the detector. By imposing equivalent criteria on the event selection, these losses are made approximately symmetrical between the two decay modes in each beam, and the correction for any residual difference between these effects in the two beams is obtained by overlaying good events with random triggers. Finally, there are systematic uncertainties associated with the background subtractions, the corrections, and the knowledge of the relative energy scale of the four modes.

The K_L and K_S beams

The K_L beam is generated by 450 GeV protons from the CERN Super Proton Synchrotron (SPS) striking a target located 120 m from the final collimator and the beginning of the fiducial region. A small contamination of K_S decays at large angles in the K_L beam coming from collimator rescattering had been seen in the previous measurement¹⁾ [2].

¹⁾ This required the first 10 m of the fiducial region to be omitted from the analysis, a reduction of 20% in statistics.

This contamination was removed by the introduction of a third, intermediate collimator designed to shield the bore of the final collimator from the debris coming off the edges of the defining collimator.

The K_S target station is movable throughout the 50 m evacuated fiducial region. The end of the single K_S collimator is located 7 m from the target and is followed by an anti-counter with a lead converter in front to define the beginning of the acceptance region for K_S decays. The position of this anti-counter is used to fix the energy scale for neutral decays with a precision of 10^{-3} with respect to the charged decay energy scale. In reference [2] both beams were generated by 450 GeV protons incident at 3.6 mrad on the target, and the measured K_S energy spectrum was harder than the K_L spectrum. This difference resulted in a systematic uncertainty in R equal to three times the uncertainty in the relative energy scales between the charged and neutral decays. To be less sensitive to this uncertainty, the difference in spectra is reduced by using protons of 450 GeV at 2.5 mrad for the K_L beam and of 360 GeV at 4.5 mrad for the K_S beam. This reduces the uncertainty on R to 1.2 times the corresponding uncertainty in the energy scale. The ratio of the spectra is shown in figure 2, and compared with that for reference [2].

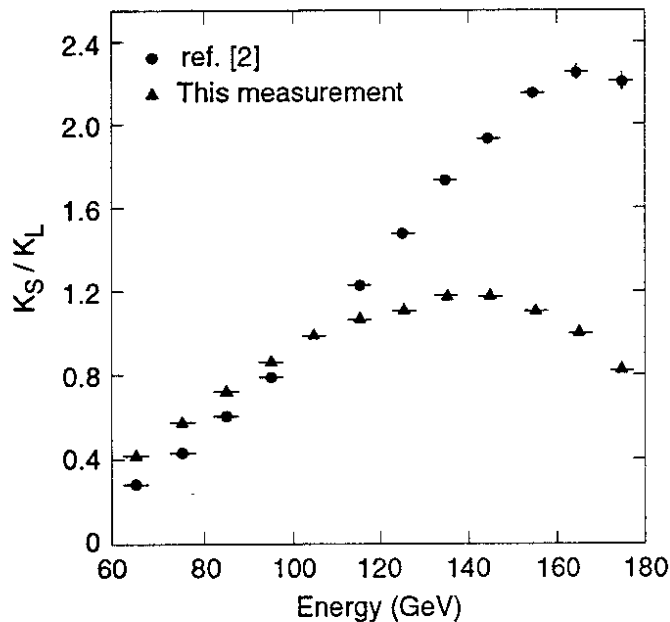


Figure 2: The ratio of the decay energy spectrum of the K_S beam to that of the K_L beam for these data (triangles) compared with the same ratio for the earlier measurement [2].

The K_L and K_S neutral beams pass in vacuum through the fiducial region and through all detector elements to a beam dump at 133 m from the final K_L collimator. At 95 m, a 1 mm thick window, made from impregnated Kevlar fibres, separates the vacuum from the helium volume containing the wire chambers. The beam is transported through the helium tank and the detector in a pipe varying from 16 cm to 19 cm in diameter. The K_L and K_S beam cones are slightly different in angle and size. The respective beam spots at the electromagnetic calorimeter have a 4 cm radius for K_L and from 4 cm to 6.5 cm radius for K_S , depending on the target station position. The beam intensity is adjusted so as to give similar activity in the detector for the two beams with a singles rate of 100 kHz. Typically 10^{11} protons per burst of 2.5 seconds duration are incident on the target in K_L running and 3×10^7 protons in K_S running.

The Detector

The detector is based on calorimetry and wire chambers, and is designed for high efficiency and large acceptance with the $2\pi^0$ and $\pi^+\pi^-$ decays recorded concurrently. The main features of the detector are:

- i) Two wire chambers placed 23 m apart in a helium tank immediately following the vacuum tank to measure the positions of the charged tracks to a precision of $\simeq 0.5$ mm per projection.
- ii) A large ($2.4 \text{ m} \times 2.4 \text{ m} \times 25$ radiation lengths) liquid-argon/lead sandwich electromagnetic calorimeter with readout organized in alternating orthogonal strips and separated into front and back halves. The resolution for photons of energy E (GeV) after calibration is $\sigma(E) = \sqrt{(0.14^2 + 0.075^2 E + 0.005^2 E^2)}$, and the position resolution is $\simeq 0.5$ mm.
- iii) An iron/scintillator hadron calorimeter consisting of orthogonal strips of scintillator separated by 2.5 cm of iron with 1.2 m total iron thickness. The resolution for pions of energy E (GeV) is $\sigma(E) = 0.65\sqrt{E}$ when used in conjunction with the liquid-argon calorimeter.

Triggers are initiated by a scintillator hodoscope in front of the liquid-argon calorimeter for decays involving charged particles, and by a hodoscope in the liquid argon, placed after 12.5 radiation lengths, for neutral pion decays. These hodoscope triggers require a coincidence in opposite quadrants for charged decays and a left/right coincidence for neutral decays. Particles outside the acceptance of the calorimeters are vetoed on-line by four rings of anti-counters surrounding the decay region. Muons from $K_{\mu 3}$ decays and pion decays in flight are vetoed by a series of anti-counters placed between iron walls behind the hadron calorimeter. The trigger further discriminates against three-body decays using: the longitudinal shower development for K_{e3} events, extra photons seen in the calorimeter, the reconstructed neutral decay vertex for $3\pi^0$ events, and the centre of gravity or the kaon direction relative to the beam axis for both charged and neutral decays. The trigger efficiency is monitored continuously using an event sample taken with relaxed trigger conditions. Typically in K_L an initial 20 kHz cross-coincidence rate is reduced to 500 Hz for events written to tape.

New components were added to the detector for the 1988 and 1989 runs to assist in the identification and rejection of background. A four-chamber transition radiation detector (TRD) [6] was placed between the second wire chamber and the charged trigger hodoscope. This provides additional electron/pion discrimination, which is used to verify the subtraction of the K_{e3} background in charged K_L decays as well as to understand better the residual non- K_{e3} background in this decay mode (see below). For the latter part of the data sample the TRD has been included in the trigger, reducing the on-line loss of $\pi^+\pi^-$ decays from 2% to a negligible level. This allows an additional check that the previous K_{e3} trigger cut does not incur losses of $\pi^+\pi^-$ events beyond that of the off-line K_{e3} rejection. The number of planes of muon counters was increased from two to four to allow a sample of stopping muons to be recorded to check the $K_{\mu 3}$ background subtraction.

In order to improve the control over and understanding of the effects of accidental activity in the detector, new elements were added in 1989. The wire-chamber electronic noise was significantly reduced and the readout was expanded from four to eight hits per chamber, for a better understanding of losses from spurious hits. The random trigger selection measures the accidental activity in the 1989 data sample by delaying a downscaled

trigger from a monitor in the neutral beam by²⁾ $69 \mu\text{s}$ instead of the $5 \mu\text{s}$ used previously. This more accurately records in the random events the accidental activity seen by good events. Finally, zero-cross TDCs are used on groups of eight calorimeter signals to identify out-of-time calorimetric activity.

Data selection

Candidates for the $2\pi^0$ decays are selected from those events with a reconstructed energy in the electromagnetic calorimeter between 60 and 180 GeV and with a reconstructed vertex between 2.1 m and 48.9 m from the position of the final K_L collimator. Candidates for the $\pi^+\pi^-$ decays are selected from events using the same energy and vertex cuts, where these variables are calculated from the reconstructed tracks in the wire chambers and the ratio of the calorimetric energies of the charged tracks. Details of the reconstruction and calibration procedures may be found in reference [4]. Additional cuts are required to remove backgrounds and to minimize systematic errors. In all cases, these cuts have been chosen to be more severe than those used in the trigger.

The final sample of $2\pi^0$ events is required to have exactly four reconstructed energy clusters (photons) in the electromagnetic calorimeter, each with energy between 3 and 100 GeV. These four photons are required to be at least 5 cm apart, and to have an impact point on the calorimeter at least 16 cm from the beam axis (4 cm from the edge of the central hole in the calorimeter). The centre of gravity of the energy deposition in the calorimeter is required to be less than 10 cm from the beam axis. Finally, the first wire chamber is required to have no reconstructed space points.

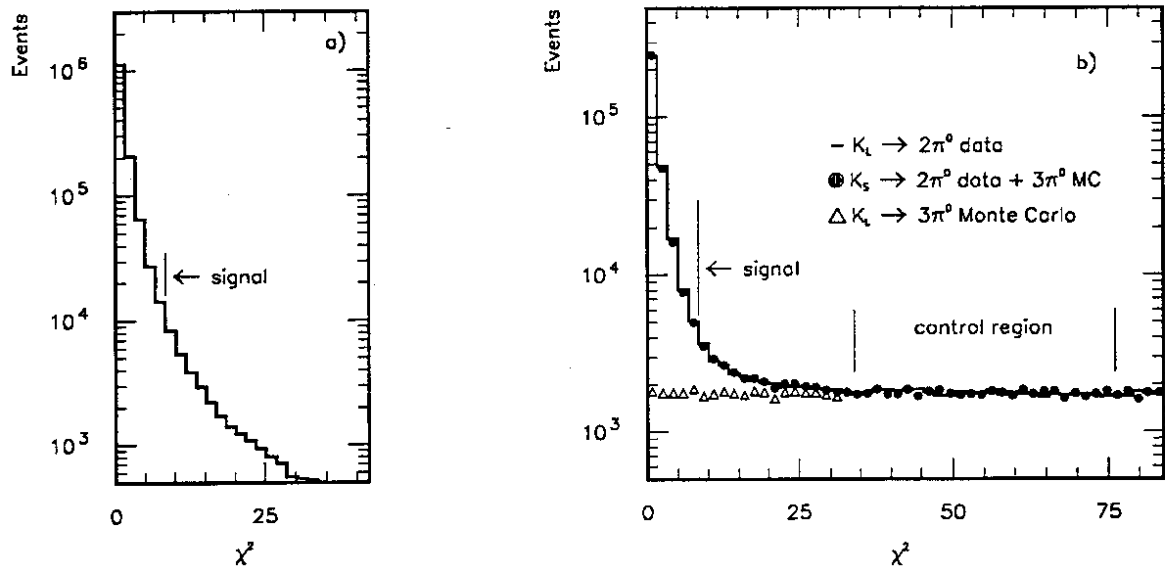


Figure 3: The distributions of (a) $K_S \rightarrow 2\pi^0$ events and (b) $K_L \rightarrow 2\pi^0$ events as a function of the χ^2 of the two π^0 masses. The $K_S \rightarrow 2\pi^0$ events (filled circles) are also included in (b), where they have been combined with the $3\pi^0$ Monte Carlo events and normalized to K_L . The $3\pi^0$ Monte Carlo events (triangles) are shown alone for $\chi^2 < 30$.

²⁾ This is three times the SPS period of $23 \mu\text{s}$ and is equal to the period of the slow resonant proton beam extraction.

The background remaining from $K_L \rightarrow 3\pi^0$ decays in which two of the six photons escaped detection in the calorimeter and the anti-counters is subtracted using a χ^2 variable constructed from the sum and difference of the masses of the two π^0 candidates. The mass resolution used for this χ^2 varies as a function of the energy of the least energetic photon. The distributions of K_S and K_L events as a function of χ^2 are shown in figures 3a and 3b. The $3\pi^0$ background is flat in this variable, as can be seen by the distribution of $3\pi^0$ Monte Carlo events shown in figure 3b. The π^0 mass resolution agrees well between K_S and K_L , which is shown in figure 3b where K_S summed together with the $3\pi^0$ Monte Carlo events is superimposed on K_L . A cut is chosen at 8.4, and various control regions are used, for example from 34 to 76, to give a flat extrapolation of the background in each energy and vertex bin. The average background subtracted is 2.7% ($< 0.1\%$) in K_L (K_S), as given in table 1, and the corresponding loss of $2\pi^0$ events is 3%, as measured in K_S .

Table 1: Number of events after background subtraction and background fractions

Decay mode	Number of events	Total background (%)
$K_L \rightarrow 2\pi^0$	319 000	2.67
$K_L \rightarrow \pi^+\pi^-$	847 000	0.63
$K_S \rightarrow 2\pi^0$	1 322 000	0.07
$K_S \rightarrow \pi^+\pi^-$	3 241 000	0.03

The $\pi^+\pi^-$ sample is required to have exactly two reconstructed space points in the first wire chamber, and to have each track in the second wire chamber greater than 18 cm from the beam axis. To be accepted as coming from a common vertex, the closest distance of approach of the two tracks is required to be less than 2.5 cm; the r.m.s. error on this distance is typically 0.3 cm. Events with a coincidence in the first two muon planes are removed.

In contrast to the $2\pi^0$ decays with only one source of background, the $\pi^+\pi^-$ decays have several. Potential contamination from $\Lambda \rightarrow p\pi$ decays is removed by requiring that the ratio of the energies of the charged particles, as measured in the calorimeters, be between 0.4 and 2.5. The reconstructed kaon mass is required to be within 2.1 standard deviations ($\sigma_{m_{\pi^+\pi^-}} \approx 20$ MeV) of the nominal value. The remaining background in the K_S data is $< 0.1\%$, predominantly due to neutron interactions in the K_S anti-counter, which is removed by extrapolating events from a mass region above the kaon mass (see the description below for the K_L backgrounds). In K_L , much of the semi-leptonic, $\pi^+\pi^-\pi^0$ and direct $\pi^+\pi^-\gamma$ backgrounds are rejected by the kaon mass cut. Events with additional energy clusters in the electromagnetic calorimeter (photons from $\pi^+\pi^-\pi^0$ and $\pi^+\pi^-\gamma$ decays) outside the pion showers are rejected. Most of the remaining K_{e3} decays are removed by an electron rejection cut which requires that the energy deposition of each track in the first 13 radiation lengths of the electromagnetic calorimeter be less than four times the energy deposition in the hadron calorimeter. The combination of the track energy-ratio cut and the K_{e3} cut rejects about 40% of the original $\pi^+\pi^-$ sample.

After all these cuts a small residual background remains in K_L . For the $\pi^+\pi^-$ decays, the decay plane should contain the production target (allowing for measurement errors and multiple scattering), whereas in general this is not true for the three-body decays.

The background can thus be estimated by studying the distribution of the perpendicular distance (d_t) from the decay plane to the target centre, geometrically scaled for the K_S data in order to compare directly with the K_L data. These distributions are shown in figures 4a and 4b. The signal region is taken as $d_t < 5$ cm, and the remaining background is estimated using events in a control region of $6 \text{ cm} < d_t < 11$ cm. There are four different contributions to the residual background in the signal region. These different background components are either directly subtracted, or extrapolated from the control to signal regions.

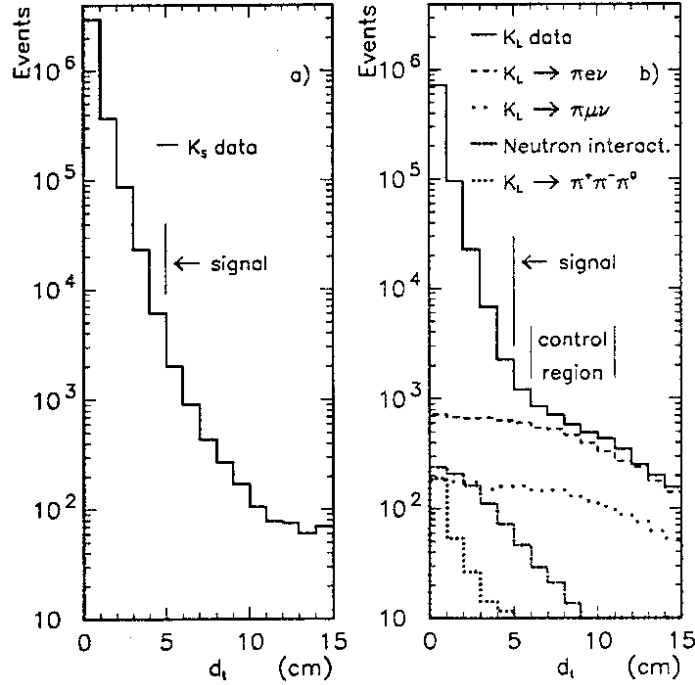


Figure 4: The distributions of (a) $K_S \rightarrow \pi^+\pi^-$ events and (b) $K_L \rightarrow \pi^+\pi^-$ events as a function of d_t , the perpendicular distance of the target from the decay plane. The dashed curves show the distributions expected from each source of background in the K_L data from three-body decays and neutron interactions.

Before subtracting the various background components, both the signal and control regions are first corrected for $\pi^+\pi^-\pi^0$, $\pi^+\pi^-\gamma$, and neutron-induced background events. Those $\pi^+\pi^-\pi^0$ and $\pi^+\pi^-\gamma$ events that remain unidentified because of the overlay of a photon and a pion shower are removed statistically by subtracting the number of events with a visible photon falling in an area just outside the hadronic shower of a pion track. The size of this background is 0.04% in the K_L beam. There is also a small background of pion pairs with a broad mass spectrum generated by neutron interactions on the residual gas in the fiducial region³⁾, or in the K_S anti-counter. A Monte Carlo was developed using neutron interaction data, and it reproduces the observed energy, mass, vertex, and d_t distributions of the neutron interactions. This is used to subtract events under the kaon mass peak, normalizing to events with mass from 0.65 to 1.0 GeV, and removes 0.09% (0.03%) of events in K_L (K_S).

The dominant remaining background is due to K_{e3} events. The fraction of K_{e3} in the control region is established using the track response in the TRD, and can be cross-checked

³⁾ For the present measurement, the residual pressure sometimes reached 3×10^{-2} Torr, a factor of 10 larger than in reference [2].

with the shower width in the liquid-argon calorimeter. The K_{e3} extrapolation factor from the control region into the signal region is determined using a sample of K_{e3} decays, where all of the $\pi^+\pi^-$ cuts are applied except the electron rejection cut which is replaced by electron selection criteria using the TRD and shower width. The K_{e3} subtraction is 0.40%.

There remains a background of $K_{\mu3}$ events, which are identified in the control region using the characteristic signature of a catastrophic energy loss in a single strip of the hadron calorimeter. The $K_{\mu3}$ background level and extrapolation are simulated by Monte Carlo. This Monte Carlo was developed for the previous measurement [2] using a special run where $K_{\mu3}$ events were selected with the muon veto. The Monte Carlo was further tested, for the present measurement, with $K_{\mu3}$ events where the muon stops between the second and third plane in the muon veto. The $K_{\mu3}$ background is 0.10%. The total background in the $K_L \rightarrow \pi^+\pi^-$ channel is 0.63%, and the various components are shown in figure 4b and summarized in table 2.

Table 2: Contributions to the K_L charged decay background

$K_L \rightarrow \pi^+\pi^-$ background	
Source	Contribution (%)
$\pi^+\pi^-\pi^0$	0.04
$\pi e\nu$	0.40
$\pi\mu\nu$	0.10
Neutron interactions	0.09

The number of events remaining after all cuts for each of the four modes, together with the subtracted background, is shown in table 1. The data are analysed in bins of 10 GeV in energy and 3.6 m in vertex position, the background is subtracted from each bin, and the double ratio is calculated separately for each of 37 self-contained data sets consisting of a cycle of K_S and K_L data taking. The weighted average of these results⁴⁾ for R is 0.9829 ± 0.0024 .

Corrections, Systematic Errors, and Systematic Checks

This result needs to be corrected for a number of small effects. The specific virtue of this method of measuring R is that the acceptance for K_S and K_L events are nearly equal, such that the acceptance correction to R is quite small. This correction, applied bin by bin, is calculated by Monte Carlo, and accounts for differences in beam divergence of the two beams, for the effects of resolution smearing of the different spectra, for finite bin-size effects, and for the difference in losses between neutral and charged decays from kaons which scattered in the K_S collimator or anti-counter. The acceptance correction, not including the correction for K_S scattering, increases the value of R by 0.0053. The correction for K_S scattering decreases the value of R by 0.0039, leading to a net acceptance correction of 0.0014 ± 0.0009 (stat.). The K_S anti-counter has a different efficiency for $2\pi^0$ and $\pi^+\pi^-$ decays owing to the four-photon conversion probability and the effective distance between the lead and scintillator. This leads to a correction which increases R by 0.0039. The efficiency of the trigger can be measured by studying events for which

⁴⁾ The corresponding value for the 1988 sample alone is 0.983 ± 0.004 , in agreement with the value presented in reference [7]

the trigger restrictions are relaxed. All trigger components were 100% efficient within statistical uncertainty, except for the processor used to calculate the $2\pi^0$ vertex, which is measured to be $\sim 99.8\%$ efficient and slightly different for K_S and K_L . This leads to a correction increasing R by 0.0012 ± 0.0002 (stat.). Finally, the net correction for the $\sim 3\%$ losses of events in each decay mode through additional accidental activity in the detector is measured by overlaying events with information obtained by triggering the detector randomly at a frequency proportional to the beam intensity. This correction is performed bin by bin where events lost (gained) after overlay are added to (removed from) each bin. This decreases R by 0.0016 ± 0.0007 (stat.). The errors on these quantities arise mainly from the limited statistics available in the various control samples.

The main sources of systematic error are summarized in table 3. The uncertainty for the $K_L \rightarrow 2\pi^0$ background is derived from the $3\pi^0$ Monte Carlo, which demonstrates that a flat extrapolation in χ^2 from the control to the signal region is correct to better than 5%. For the $K_L \rightarrow \pi^+\pi^-$ background, the uncertainty arises from both the uncertainty in the extrapolation factors for each of the components removed from the signal as well as from the limit on any residual $\pi^+\pi^-\pi^0$ component. The uncertainty in the accidental activity correction is obtained by studying the stability of the corrected value of R when varying cuts sensitive to accidental activity. As can be seen in figure 5a for K_L , the net losses increase with beam intensity and are nearly identical for the two decay modes. Figure 5b shows R after correction for accidentals as a function of intensity in the K_L beam.

Table 3: Sources and magnitude of corrections and systematic uncertainty in the double ratio R

Source	Correction (%)	Systematic uncertainty (%)
Background to $K_L \rightarrow 2\pi^0$	2.67	0.13
Background to $K_L \rightarrow \pi^+\pi^-$	0.63	0.10
Accidental activity	0.16	0.14
Energy scale calibration and stability		0.13
Trigger and K_S anti-counter inefficiencies	0.51	0.09
Monte Carlo acceptance	0.14	0.10
Wire chamber inefficiency		0.10
Total systematic uncertainty		0.30

Small variations of the calorimetric energy measurements have been observed, primarily in K_L , for events waiting in an analogue memory for a previous event to be digitized and read out. The effects of these variations have to a large extent been minimized by a pedestal correction based on the time spent in the analogue memory. Residual effects are implicitly removed by the overlay correction for accidentals. These corrections have been extensively studied using the dependence of the physical quantities, such as the π^0 mass for neutral events and the kaon mass for charged events. For the subset of the data where the measurement of the time spent in the analogue memory is available, there remains a difference in the charged to neutral ratio of events in K_L according to whether or not the events wait. This ratio is 2.646 ± 0.011 for events that wait and 2.692 ± 0.009 for those events that do not wait, where the errors are purely statistical. Within the systematic

error quoted below, no loss of events due to trigger, read-out or analysis cuts has been found to be correlated with the waiting time; therefore all events have been used. As shown in figure 5b, there is also no evidence for a dependence of R on intensity, to which the event waiting time is correlated.

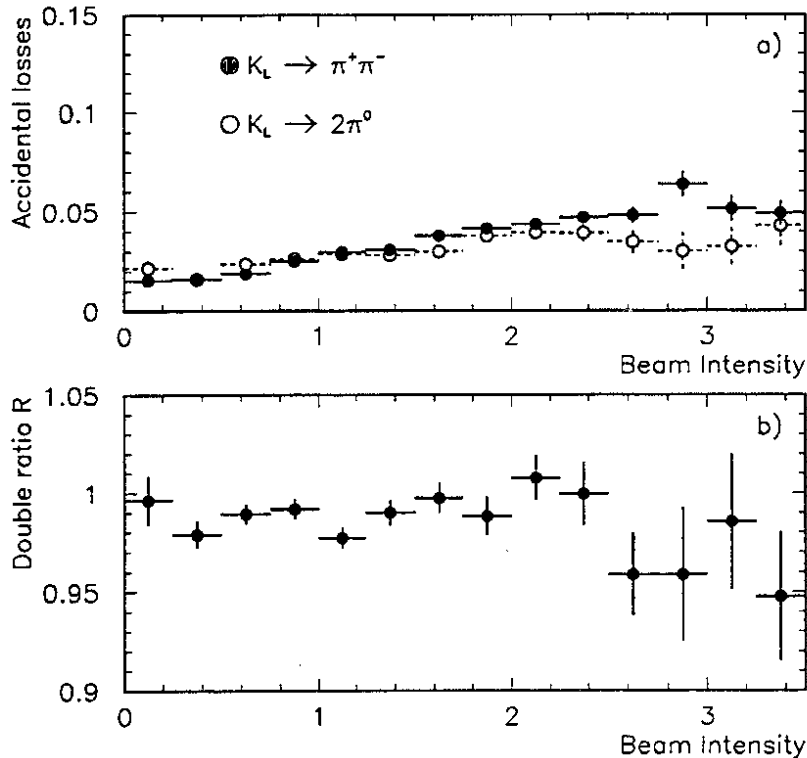


Figure 5: (a) The average accidental corrections from the overlay of random events for $K_L \rightarrow \pi^+\pi^-$ and $K_L \rightarrow \pi^0\pi^0$ as a function of the instantaneous beam intensity in K_L . (b) The double ratio R as a function of the K_L beam intensity. The intensity is normalized to the mean intensity.

There is a systematic uncertainty associated with the knowledge of the relative energy scales between each of the four decay modes. By fitting to the anti-counter position in K_S , the $2\pi^0$ energy scale is fixed and the kaon energy scale for $\pi^+\pi^-$ decays, which is established by the geometry of the wire chambers, is checked. The stability of the energy calibration is monitored, both in time and between the two beam modes, using the reconstructed kaon mass for the $\pi^+\pi^-$ decays, and by comparing the vertex positions reconstructed from the wire chambers and the electromagnetic calorimeter for $2\pi^0$ decays in which one of the π^0 undergoes a Dalitz decay and for $K_L \rightarrow \pi^+\pi^-\pi^0$ decays. The combined systematic uncertainty in R from the energy scale, stability, and any residual non-linearity is 0.0013.

The systematic error for the trigger is statistical in nature, limited by the number of events taken with relaxed trigger conditions. A potential systematic effect due to accidental activity, not covered by the overlay correction, is an accidental trigger followed by a good neutral or charged decay. Some of these events could survive both trigger and off-line cuts and create an asymmetry. Using the zero-cross TDCs the rate of good events with calorimetric signals which are late with respect to their trigger time is measured to be

$1-2 \times 10^{-4}$ for the different decay modes, with no discernable asymmetry at the 10^{-4} level. The systematic error on the trigger efficiency and the correction for the K_S anti-counter inefficiency is estimated to be 0.0009.

A systematic error could arise if the wire chamber inefficiency changed with beam conditions. Owing to the redundancy obtained with four planes per chamber, the inefficiency is small. The losses in the first chamber are about 0.05% in both beams; in the second chamber about 0.3% of events are lost in K_L runs and 0.1% in K_S runs. These losses are estimated from K_{e3} and $K_S \rightarrow \pi^+\pi^-$ data, where the event is defined by only the calorimeter and one chamber. This inefficiency is entirely compatible with the expected losses from dead channels, which is symmetric between K_S and K_L , and from accidental activity, for which a correction has been made. There is therefore no correction to R due to chamber inefficiency within an estimated systematic uncertainty of ± 0.001 .

As previously mentioned, approximately 40% of good $K \rightarrow \pi^+\pi^-$ decays are removed by the track energy-ratio and K_{e3} cuts. The track energy-ratio cut has been varied so that the loss of $\pi^+\pi^-$ decays is changed by $\pm 10\%$. Variations of the double ratio are all within 0.1%. Similarly, alternative electron rejection cuts using the TRD in combination with a calorimetric cut have been applied to half of the data sample. These cuts allow the nominal 20% loss of $\pi^+\pi^-$ events from the electron rejection to be reduced to between $\sim 1\%$ and 10%, with a corresponding total background subtraction from 1.6% to 0.6%. The resulting variations of the double ratio are well within the $\sim 0.1\%$ statistical uncertainty. In addition, the K_{e3} background subtraction itself can be checked by applying a TRD cut in addition to the standard electron rejection. For a TRD cut which reduces by a factor of three the remaining K_{e3} background and rejects only 0.4% of $\pi^+\pi^-$ events, the change in the double ratio is 0.02%.

The final result for R is $0.9878 \pm 0.0026 \pm 0.0030$, where the first error is statistical and the second is systematic. This represents a net correction of only 0.0049 relative to the weighted average given above. A full discussion of the systematic investigation of the result will be found in a complete description of the experiment to be published [5].

Conclusions

The result of this measurement of R gives $\text{Re } \epsilon'/\epsilon = (2.0 \pm 0.7) \times 10^{-3}$. In order to combine this result with our previous result, $\text{Re } \epsilon'/\epsilon = (3.3 \pm 1.1) \times 10^{-3}$ [2], a common systematic uncertainty of 0.0028 in R must be taken into account. The averaged result for R is then 0.9862 ± 0.0039 , and the corresponding value for $\text{Re } \epsilon'/\epsilon$ is $(2.3 \pm 0.65) \times 10^{-3}$.

This result can be compared with recent measurements performed at Fermilab. These are $\text{Re } \epsilon'/\epsilon = (3.2 \pm 3.0) \times 10^{-3}$ [8] and $\text{Re } \epsilon'/\epsilon = (0.74 \pm 0.59) \times 10^{-3}$ [3]. Combining the averaged results of the two experiments gives $\text{Re } \epsilon'/\epsilon = (1.48 \pm 0.43) \times 10^{-3}$, more than three standard deviations from zero. The probability for these respective measurements to be consistent with each other and agree with the overall average is 9%. The results of these experiments provide evidence for direct CP violation at a level consistent with the expectations of the Standard Model with a top-quark mass in the region of 150 GeV [9].

Acknowledgements

We would like to thank the technical staff of the participating laboratories, universities, and affiliated computing centres for their dedicated efforts in the design, construction, and maintenance of the beam, detector, and data acquisition, and in the processing of the data. We would especially like to thank the following: F. Blin, M. Clément, G. Dubail,

G. Dubois, G. Kessler, G. Laverrière, P. LeCosec and M. Marin from *CERN*; D.J. Candlin, A. Main, P. McInnes and J. Muir from the *University of Edinburgh*; K. H. Geib, R. Gläser and A. Weissbeck from the *Universität Mainz*; G. Barrand, R. Bernier, B. Chase, J. P. Coulon, M. Dialinas, E. Plaige, J. P. Richer and P. Roudier from the *Laboratoire de l'Accélérateur Linéaire*; C. Avanzini, S. Galeotti, G. Gennaro, F. Morsani, G. Pagani, D. Passuello, R. Ruberti and L. Zaccarelli from the *Dipartimento di Fisica e Sezione INFN di Pisa*; M. Roschangar and R. Seibert from the *Universität Siegen*.

References

- [1] Particle Data Group, K. Hikasa *et al.*, *Phys. Rev. D* **45** (1992) 1.
- [2] H. Burkhardt *et al.*, *Phys. Lett. B* **206** (1988) 169.
- [3] L.K. Gibbons *et al.*, *Phys. Rev. Lett.* **70** (1993) 1203.
- [4] H. Burkhardt *et al.*, *Nucl. Instrum. Meth. A* **268** (1988) 116.
- [5] G.D. Barr *et al.*, A measurement of direct CP violation in the neutral kaon system, to be published.
- [6] G.D. Barr *et al.*, *Nucl. Instrum. Meth. A* **294** (1990) 465.
- [7] G.D. Barr, CERN–Edinburgh–Mainz–Orsay–Pisa–Siegen Collaboration, *Proc. Joint Int. Lepton–Photon Symposium and Europhysics Conf. on High Energy Physics, Geneva, 1991* (World Scientific, Singapore, 1992), p. 179.
- [8] M. Woods *et al.*, *Phys. Rev. Lett.* **60** (1988) 1695.
- [9] M. Ciuchini, E. Franco, G. Martinelli and L. Reina, *Phys. Lett. B* **301** (1993) 263; A.J. Buras, M. Jamin and M.E. Lautenbacher, preprint CERN-TH-6821/93 (MPI-Ph/93-11, TUM-T31-35/93).

DISPLAY

1

Report Number = UAB-FT-321;C93-07-30
Author(AF) = Masso, Eduard (Barcelona, Autonoma U.)
Title = New constraints on galactic dark matter.
Date = Aug 1993
KEK Accession Number = 93-12-315

2

Report Number = LNGS-93-85;C93-07-06
Author(AF) = Berezinsky, V. (INFN, Aquila;Moscow, INR (4383)
Ph: 7 95 3340066)
Title = Neutrinos as dark matter and neutrinos from dark
matter.
Date = Nov 1993
KEK Accession Number = 93-12-113

3

Report Number = LNGS-93-83;C93-09-06.4
Author(AF) = Bacci, C.;Belli, P.;Bernabei, R.;Changjiang, Dai
;Linkai, Ding;Di Nicolantonio, W.;Gaillard, E.;G
erbier, G.;Haohuai, Kuang;Incicchitti, A.;Mallet

XPRI 英字 0 MS-DOS 94-01-20 Thu 14:42
■ 英数 PRA

93-11-014

10-191

06-088

93-07-427

93-11-330

93-06-537

93-04-163